

Joint Plasticity Learning for Camera Incremental Person Re-Identification

Zexian Yang^{1,2} Dayan Wu^{1*} Bo Li^{1,2} Weiping Wang^{1,2}

¹Institute of Information Engineering, Chinese Academy of Sciences

²School of Cyber Security, University of Chinese Academy of Sciences

{yangzexian, wudayan, libo, wangweiping}@iie.ac.cn

Abstract

Recently, incremental learning for person re-identification receives increasing attention, which is considered a more practical setting in real-world applications. However, the existing works make the strong assumption that the cameras are fixed and the new-emerging data is class-disjoint from previous classes. In this paper, we focus on a new and more practical task, namely Camera Incremental person ReID (CIP-ReID). CIP-ReID requires ReID models to continuously learn informative representations without forgetting the previously learned ones only through the data from newly installed cameras. This is challenging as the new data only have local supervision in new cameras with no access to the old data due to privacy issues, and they may also contain persons seen by previous cameras. To address this problem, we propose a non-exemplar-based framework, named JPL-ReID. JPL-ReID first adopts a one-vs-all detector to discover persons who have been presented in previous cameras. To maintain learned representations, JPL-ReID utilizes a similarity distillation strategy with no previous training data available. Simultaneously, JPL-ReID is capable of learning new knowledge to improve the generalization ability using a Joint Plasticity Learning objective. The comprehensive experimental results on two datasets demonstrate that our proposed method significantly outperforms the comparative methods and can achieve state-of-the-art results with remarkable advantages.

1. Introduction

Person re-identification (ReID) aims to match the same identity across different camera views. Thanks to the outstanding advance in deep learning technology [22, 14, 26], we have recently seen many state-of-the-art performances of this task [7, 38]. Nevertheless, most of those [36, 23, 29]

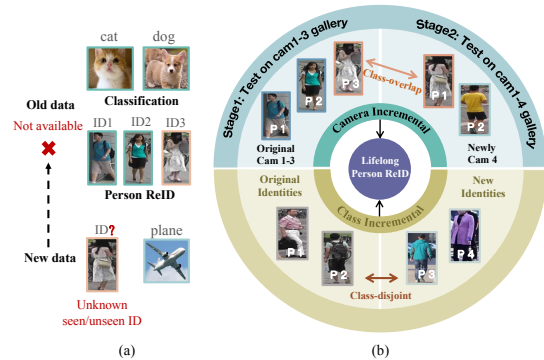


Figure 1. Illustration of (a) Class-overlap issue: Real-World data with unknown seen person. (b) Our proposed camera incremental vs class incremental. New data are labeled independently in the new stage and they may contain identities have been seen before. At each stage, the model will be tested on the gallery of all encountered cameras.

assume the person ReID model is trained with a fixed dataset, which inevitably hinders its scalability to real-world applications. In practice, ever-expanding data captured from surveillance systems every day pose a realistic demand to person ReID task, that is, to continuously improve the generalization of person ReID model with increasing new data.

To meet this demand, incremental learning for person ReID (ILReID) has recently emerged as a practical solution. ILReID follows the standard class-incremental training pipeline where new data is class-disjoint from the old ones. In contrast to the class-incremental classification task [20, 9, 15, 37], performing incremental learning for person ReID [35] poses additional challenges. The first one is that the training set and test set classes are disjoint, which is viewed as a zero-shot problem. Another *overlooked* problem is that the person ReID dataset is labeled without specific identity information (only number), making it difficult to identify whether the new data belongs to a seen or unseen class (see Fig. 1(a)).

Recent efforts [27, 11, 18] have been devoted to seeking a balance between catastrophic forgetting [19] and gener-

*Corresponding author.

alization. They mainly focus on the scenarios where new identities keep increasing in fixed camera systems. However, contemporary surveillance systems are under dynamic changing, which means cameras can be added or removed from surveillance systems at any time. Motivated by this gap, we focus on a new and more practical task, named **Camera Incremental Person ReID (CIP-ReID)**. As illustrated in Fig. 1(b), CIP-ReID aims to optimize the model when one or more cameras are introduced in the existing surveillance systems. Furthermore, we expect the model can continuously learn more scalable feature representations by obtaining knowledge from new data (termed as plasticity learning).

Different from previous class-incremental and lifelong person ReID work, CIP-ReID is characterized by the following aspects. **1) Class overlap setup.** Imagine that a new camera is installed in the community, old IDs (the old neighbors) and new ones (the new neighbors and visitors) will both exist. **2) Local supervision.** Given that the cross-camera pairwise labels are missing due to privacy concern, at each stage, the identity labels can *only* be annotated within the new camera independently. In this case, we are supposed to tackle the label alignment for the unknown overlapping classes. **3) Cross-camera domain gap.** Variations of lighting, viewpoint and background of new cameras will result in a cross-camera domain gap. To sum up, the challenge of CIP-ReID is how to overcome the class-overlap and domain gap issues with local supervision and how to further boost the model generalization ability.

To meet the aforementioned challenges, we first present a simple baseline to set a new lower-bound, and further propose our new framework for CIP-ReID task. Firstly, considering that the new data may contain identities seen in previous stages, we introduce a One-Vs-All (OVA) classifier [21] that can classify target samples into either seen or unseen categories. Based on the OVA classifier, we further propose an ID-wise label assignment strategy to align each local ID to one global pseudo label. Secondly, to mitigate the domain gap between the original cameras and the new ones, we propose a prototype-based joint plasticity learning method. This method memorizes the class mean instead of raw data as prototypes and then enables the samples in the new camera to pull or push away from the augmented embedding based on the prototypes. Moreover, to avoid catastrophic forgetting, we adopt a similarity distillation loss term together with the well-known knowledge distillation [8] loss function to maintain the similarity relation in feature space. In conclusion, our contributions can be summarized as follows:

- We introduce a novel yet more practical ReID task, named *Camera Incremental Person ReID (CIP-ReID)*. The task is fundamentally different from the existing class-incremental and lifelong person ReID tasks.

It demands continuously learning more generalisable representations through data from newly installed cameras only with local supervision.

- We identify the peculiar class-overlap issue in incremental learning for person ReID and carefully design a new framework for CIP-ReID, named JPL-ReID. We propose a pseudo label assignment scheme and a joint plasticity learning method for tackling the classes-overlap issue and learning fine-grained camera-invariant features.
- For extensive assessment, we build a simple baseline in addition to JPL-ReID to tackle CIP-ReID. Experimental results show that the proposed approach gains significant advantages over the comparative methods.

2. Related Work

Person Re-identification. Fully supervised person ReID methods [17, 24] focus on learning scalable representations to metric the similarity among the unseen classes while using fully inter-camera labeled data. Considering that it is expensive to annotate a large scale dataset, some work attempt to train a model in an unsupervised manner [30, 31, 28], including unsupervised domain adaptation [2, 40] and unsupervised pre-training [1, 34]. In addition to the aforementioned person ReID setups, recently proposed intra-camera supervised person ReID [4, 39] is a special semi-supervised setting. These studies consider reducing the human efforts in the process of annotating the cross-camera pairwise positive labels. They assume that annotations are independently labeled in each camera view and further discover cross-camera identities associations. However, all the above researches do not concern the fact that the data is usually imported in a stream and the fixed model cannot perform well on ever-expanding databases. In this paper, we consider addressing a new task, i.e., CIP-ReID with intra-camera supervision. Different from the intra-camera supervised person ReID, our task is more challenging as we need to establish cross-cameras ID relationships without access to previous data.

Incremental Learning for Person ReID. Incremental or lifelong learning for Person ReID is a more scalable problem that has garnered significant interest recently. Different from the well-known image-classification task, incremental learning for person ReID need to concern how to improve the generalization ability to unseen classes. Moreover, similar to few-shot learning [13, 33], the scarcity of new data is more challenging in lifelong Person ReID. The existing work [18, 27, 16, 3] mainly focus on the cross-domain incremental scenarios, they attempt to train one unified model that learns several domains in an incremental fashion and

tests the model on all encountered domains with their corresponding test sets. However, such a paradigm is insufficient to achieve comparable performance than respectively training each model on their corresponding domain. In this paper, we undertake incremental learning for person ReID based on the most realistic scenario. Suppose a community with a surveillance system installs a new camera in a certain area, people who presented in the new camera may or may not have appeared in the previous cameras, how can we utilize the data in the new camera to develop the original person ReID model.

3. Preliminary

3.1. CIP-ReID Setting

In CIP-ReID setting, the training process can be split into several stages. In the first stage, the model is trained to learn a set of classes Y^o using the data \mathcal{D}_o from the initial multiple cameras. Following the definition of incremental learning, in the incremental stage, the model will continue to be trained on a set of classes Y^n employing the training data \mathcal{D}^n from the newly installed camera. Note that the old training data \mathcal{D}^o are no longer available due to the privacy concern. Unlike other existing incremental learning methods for person ReID that enforce strict class-disjoint $Y^o \cup Y^n = \emptyset$, we assume the old classes can still occur in the new training data. Different from classification tasks, data in person re-identification tasks do not have specific attribute categories but rather ID numbers, thus we can only label local ID for the data within the new camera. For the test phase, the model will be evaluated on unseen classes from all encountered cameras. In order to evaluate the generalization ability, we will additionally test the model trained at different stages on a fixed test set.

3.2. A CIP-ReID Baseline

We first present a straightforward baseline for CIP-ReID task.

Basically, in the t -th stage ($t > 1$), our baseline model contains a deep model consists of a feature extractor $F(\theta_t)$ and an identity classifier $G(\phi_t)$ initialed by the last stage. The classifier $G(\phi_t)$ will be expanded as a unified classifier for both old classes and new classes. As a common baseline LwF [15], in addition to ReID loss (e.g. ID loss \mathcal{L}_{ID} + triplet loss $\mathcal{L}_{Triplet}$), knowledge distillation (KD) loss \mathcal{L}_{KD} are employed to prevent catastrophic forgetting, which can be formulated as:

$$\mathcal{L}_{KD} = \sum_{i \in X_t} KL(p_i^n || p_i^o) \quad (1)$$

Where $KL(\cdot)$ is the Kullback Leibler (KL) divergence distance, p_i^o and p_i^n denote the probability output of the old and new models, respectively.

To discriminate the old and new identities without accessing the old data, a straightforward method is to leverage the classification output of the old model. We assume that a smoother probability distribution indicates the sample is ambiguous. In contrast, one class with significantly higher score than the other classes, indicating that the sample may belong to this seen class. To this end, we introduce a filtering mechanism to preprocess data before training. Specifically, we feed the new samples into the frozen old model and get their corresponding softmax classification output of the old classes. Then we can find the nearest neighbor class, i.e., the class with the highest probability output, and set a threshold T to determine whether the sample is an old or new class. For samples identified as a new class, we add a new ID based on the existing old classes. As for samples classified into old classes, we directly use the old ID with the largest probability output as its pseudo label. Then we can minimize the entropy of the classifier with the global pseudo labels. The loss function can be formulated as:

$$\mathcal{L}_{ID} = \mathcal{L}_{CE}(G(F(X_t; \theta_t); \phi_t), Y'_t) \quad (2)$$

where Y'_t is the pseudo label of samples X_t , \mathcal{L}_{CE} is the cross-entropy loss function.

Overall, the optimization objective of the baseline CIP-ReID model can be formulated as:

$$\mathcal{L} = \mathcal{L}_{ID} + \mathcal{L}_{Triplet} + \mathcal{L}_{KD} \quad (3)$$

4. The Proposed approach

The filtering mechanism proposed in our baseline method is an alternative way to address the class-overlap issue. However, the manual set threshold T is not robust enough to identify old classes, mainly due to a large number of classes of person re-identification task. As more classes are incorporated into the classifier layer, the probability distribution becomes softer. Therefore, in this section, we introduce a new framework for CIP-ReID.

4.1. Overview of Framework

The framework of our method is shown in Fig. 2. The training data is input as a data stream $\mathcal{D}^t = \{(x_i^t, y_i^t) |_{i=1}^{N_t}\}$. It is noteworthy that ID labels $y_i^t \in Y^t$ are annotated intra new camera C^t in the t -th stage. The first technical novelty comes from taking advantage of One-vs-All (OVA) detector for detecting the unknown identities. Then the samples are assigned corresponding pseudo labels based on our proposed strategy, as to be detailed in section 4.2. Meanwhile, their pseudo labels are used for calculating the ID loss as well as joint plasticity loss that is detailed in section 4.3. In addition, in section 4.4, the SD loss is employed as a regular term to restrain similarity relation.

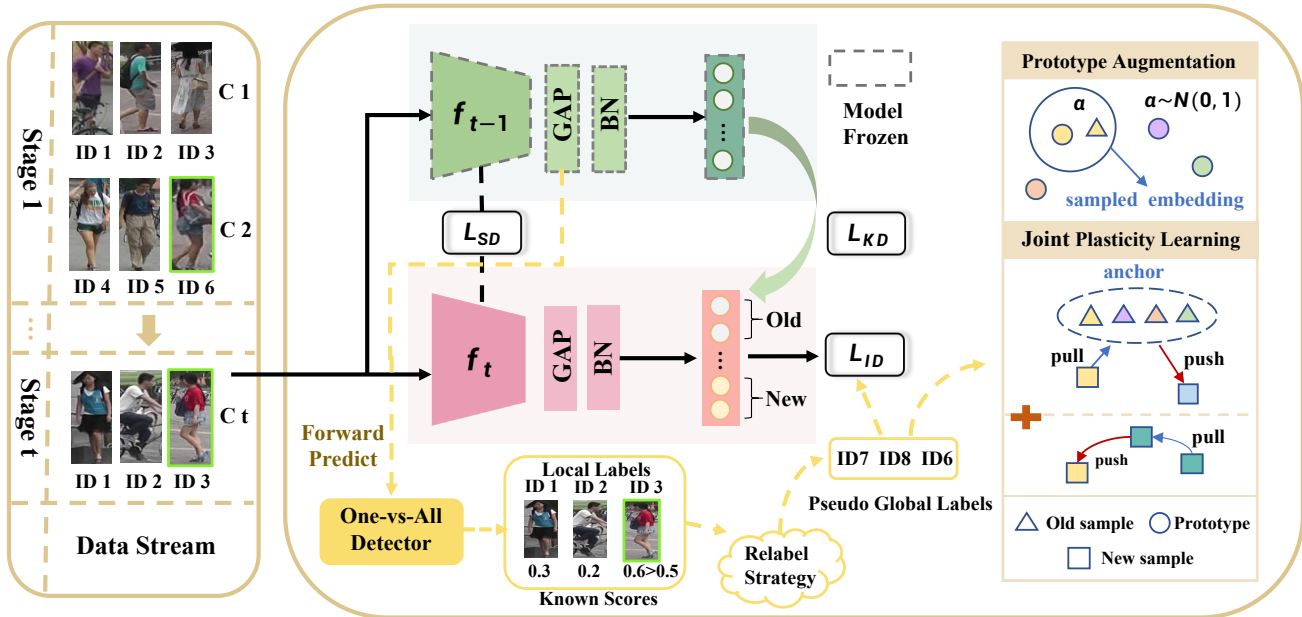


Figure 2. An overview of the proposed framework.

4.2. One-vs-All Detector for Pseudo Label Assignment

In this section, we elaborate the process of pseudo label assignment. We first describe the training of the One-vs-All detector before describing the remaining methods.

One-vs-All Detector. The One-vs-All (OVA) detector was first proposed for the open-set problem [32, 10], which aims to train a classifier to learn a boundary between in-liers and outliers for each class. Specifically, the OVA detector consists of multiple binary sub-classifiers, each of which is responsible for its class. For each sub-classifier, samples belonging to this class are trained to be positive while others are negative. Formally, we denote $p(\hat{y}^c|x)$ as the positive probability output from softmax for the class c . The optimization objective for a sample x_i within label y_i can be formulated as:

$$\mathcal{L}_{ova}(x_i, y_i) = -\log p(\hat{y}^{y_i}|x_i) - \min_{j \neq y_i} \log p(\hat{y}^j|x_i) \quad (4)$$

For more effectively learning a boundary to identify unknown identities, herein we only pick hard negative samples to compute the loss in Eq. 4. For our setup, the number of sub-classifiers at each stage corresponds to the output dimension of the identity classifier. In the inference phase, we utilize both the OVA detector and the identity classifier of the old model. We first get the nearest neighbor class according to the identity classifier output and take the corresponding score of the OVA detector. Then we set a threshold $\sigma = 0.5$ to determine whether the sample is a known or unknown class, as illustrated in Fig. 2.

Although the trained detector can identify most of the samples correctly, we empirically found that there are still some hard negative samples that will be misjudged. In other words, two images of the same class may be paradoxically predicted as a new class and an old class. Likewise, several old classes may be predicted for the same new class, resulting in additional noise in the identity classifier expansion stage. To this end, we propose a ID-wise pseudo label assignment strategy to associate the samples with the same local label to the identical pseudo global label.

ID-wise Pseudo Label Assignment Strategy. Different from the open-set problem where unsupervised data can only be labeled instance-wise, our local supervised setup is capable of ID-wise annotation. Given a batch of N training samples $\{(x_i, y_i)\}_{i=1}^N$ that follows PK sampling, i.e., $N = P \times K$, we first analyze the output of the samples with the same ID from the OVA detector, and only when the number of which predicted as an unknown category is greater than $K/2$ can we identify it as a new class otherwise old class. Then we maintain a key-value structure where each local ID y_i predicted to be a new class corresponds to a pseudo global label. For the old class samples, we still use the predicted result of the old model as their pseudo-label.

4.3. Joint Plasticity Learning

As a common practice in fully supervised person ReID [22, 6], the plasticity learning objective readily provides a camera-invariant feature representation. The plasticity learning strive to ensure the embedding distance between an anchor $F(x_a^{c_1})$ from camera c_1 and a positive $F(x_p^{c_2})$

from camera c_2 , both of which have the same identity, and maximize the embedding distance between the anchor and a negative $F(x_n^{c_3})$ of a different identity from camera c_3 , which is benefit to align feature distribution among different cameras. Formally, we have:

$$\|F(x_a^{c_1}) - F(x_p^{c_2})\|_2^2 < \|F(x_a^{c_1}) - F(x_n^{c_3})\|_2^2 \quad (5)$$

However, in our setup, we only have samples from the new camera to build the triple for intra-camera plasticity learning, which restricts the objective of cross-camera feature alignment. Inspired by [37], we perform the prototype augmentation as illustrated in Fig. 2. We do not memorize any old samples but the class center for each old class, which is assume to lie in Gaussian distribution. Then in the new stage, old class embedding is sampled based on those old prototypes with that assumption distribution:

$$embedding_c = \mu_c + \alpha * \delta \quad (6)$$

where $\alpha \sim \mathcal{N}(0, 1)$, μ_c is the mean of features that belong to old class c , δ is a scale parameter to control the uncertainty of the augmented old class embedding, it can be calculated by the average variance of features in the first stage.

Based on the augmented old class embedding, we design a joint plasticity learning method for learning camera-invariant features. On the one hand, we consider taking the augmented old class embedding as anchors, and taking new stage samples with the old class pseudo label as positive, otherwise negative. Formally, suppose the label set of old classes is denoted as \mathcal{C}_{old} , given a batch of augmented embedding $\mathcal{E} = \{embedding_{c_b}\}_{b=1}^B$, we want:

$$\begin{aligned} \mathcal{L}_{Inter} = & \sum_{c_b \in \mathcal{C}_{old}} [m + \max \|embedding_{c_b} - F(x_p^{c_t})\|_2^2 \\ & - \min \|embedding_{c_b} - F(x_n^{c_t})\|_2^2]_+ \end{aligned} \quad (7)$$

where m is margin, $[\cdot]_+$ indicates the hinge loss, $x_p^{c_t}$ and $x_n^{c_t}$ is the positive and negative sample from new camera c^t , respectively. The motivation behinds this design is to align the feature distribution between the new camera and previous cameras.

On the other hand, for samples in the new camera, we still expect to build the triple for intra-domain plasticity learning. Thus, we have:

$$\begin{aligned} \mathcal{L}_{Intra} = & \sum_{a=1}^B [m + \max \|F(x_a^{c_t}) - F(x_p^{c_t})\|_2^2 \\ & - \min \|F(x_a^{c_t}) - F(x_n^{c_t})\|_2^2]_+ \end{aligned} \quad (8)$$

Combining the objectives presented above, we reach a joint plasticity learning objective, given as:

$$\mathcal{L}_{Joint} = \lambda_1 * \mathcal{L}_{Inter} + \lambda_2 * \mathcal{L}_{Intra} \quad (9)$$

where $\lambda_1, \lambda_2 \in (0, 1)$ denote the hyper-parameters.

4.4. Similarity Distillation

The knowledge distillation loss illustrated in Eq.1 dedicates to maintaining the class-level probability distribution while weakening the distributions consistency of feature space. In fact, it is of crucial for ReID models to maintain the similarity relation have learned before. To this end, we further introduce the similarity distillation as a regular term that requires the feature similarity distribution computed by the current model to match that computed by the old model. Specifically, we feed a batch of samples $\mathcal{X} = \{(x_i^t, y_i^t)\}_{i=1}^B$ into the old model, then we calculate the cosine similarity score:

$$s_{i,j}^o = \frac{F^o(x_i^t)^T F^o(x_j^t)}{\|F^o(x_i^t)\|_2 \|F^o(x_j^t)\|_2} \quad (10)$$

where $x_i^t, x_j^t \in \mathcal{X}$, $F^o(\cdot)$ indicates the feature extractor of old model.

In the same way, we compute the similarity $s_{i,j}^n$ from the current model and the similarity distillation loss is shown as:

$$\mathcal{L}_{SD} = \sum_{i,j \in B} (s_{i,j}^o - s_{i,j}^n)^2 \quad (11)$$

Herein, the overall optimization objective to alleviate catastrophic forgetting can be formulated as:

$$\mathcal{L}_{Distill} = \mathcal{L}_{KD} + \lambda_3 * \mathcal{L}_{SD} \quad (12)$$

where $\lambda_3 \in (0, 1)$ is a hyper-parameter.

5. Experiments

5.1. Datasets and Evaluation Metrics

Datasets. We conduct extensive experiments on two large-scale person ReID datasets: Market-1501 [36] and MSMT17 [26]. To simulate the CIP-ReID setting, we split the original datasets into three separate sample sets (three stages) according to the specific camera order and generate intra-camera identity labels based on the provided annotations. In practice, a surveillance system would be set up with a batch of cameras installed first, followed by a steady stream of new ones. Thus, at the first stage, we select 4 cameras and 7 cameras for Market-1501 and MSMT17 respectively, and evenly add 1 more camera for each remaining stage. Besides, the order of new cameras and the ratio of seen and unseen persons are also unpredictable. To this end, we present additional two datasets considering different camera addition sequences and different ratios settings. The statistics of the datasets is detailed in Table 1.

Evaluation Metrics. We use the mean Average Precision (mAP) and Rank-1 accuracy for evaluation. To evaluate the

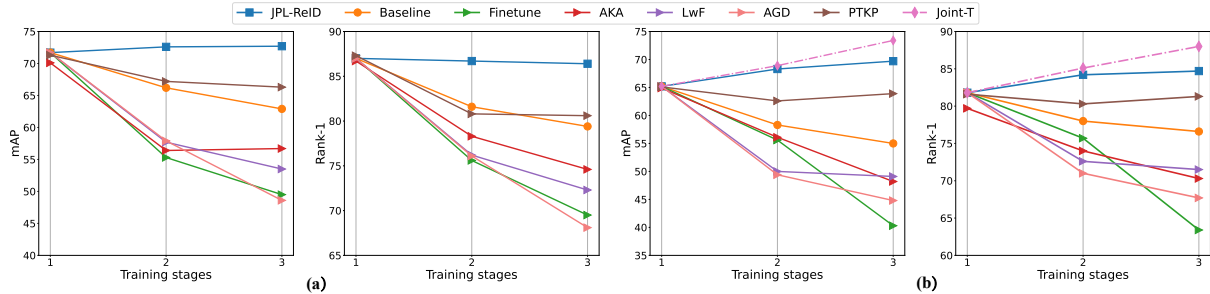


Figure 3. (a) Anti-forgetting evaluation. mAP and Rank-1 score on the original cameras (Market1501₁-stage1) during the training process. (b) Generalised performance evaluation. The model are evaluated on testing data of all cameras.

Table 1. The statistics of ReID training dataset in our experiments

Datasets	Total		Stage1		Stage2			Stage3		
	IDs	Images	CID	IDs	CID	IDs	seen/unseen ids	CID	IDs	seen/unseen ids
Market1501 ₁	684	10240	C1,3,5,6	300	C4	241	100 / 141	C2	541	288 / 253
Market1501 ₂	665	9792	C1,2,3,6	300	C4	241	110 / 131	C5	506	272 / 234
Market1501 ₃	736	10880	C1,3,5,6	600	C4	241	201 / 40	C2	541	456 / 85
MSMT17	800	12936	C1,5,7,11,13,14	600	C6	207	95 / 112	C15	254	166 / 88

incremental learning performance, we test the model on unseen classes of all encountered cameras. To evaluate the anti-forgetting ability, we test the model on unseen classes of the original cameras (the first stage). To evaluate the generalization performance more comprehensively, we further test the model on entire unseen gallery after each training stage.

5.2. Implementation Details.

For training, we choose the widely used ResNet-50 [5] as the backbone. The last layer of the network is followed by a Batch Normalization layer (BN) [12] to yield 2048-dimensional features. Adam optimizer with learning rate 3.5×10^{-4} is used. Following the few-shot learning [25] that scale learning rate during few-shot fine-tuning, the learning rate of backbone is separately set to $lr/10$ during the incremental learning stage. We train the model for 50 epochs per stage, and decrease the learning rate by $\times 0.1$ at the 25th epoch. We set the batch size to 64, including 16 identities and 4 images each identity. The number of augmented embedding corresponding to the batch size. The hyperparameter T , m , λ_1 , λ_2 and, λ_3 is set to 0.5, 0.3, 0.5, 1 and 0.9, respectively.

For comparative experiments, we run the classical incremental learning method LwF [15] and the state-of-the-art methods including AKA [18], AGD [16], and the exemplar-based method PTKP [3] on our setting. It is noteworthy that these methods are based on a class-disjoint setting, and they do not match our setting. Therefore, to implement them in our setting, they can only treat old classes as new ones. For more extensive assessment, we design some other comparative methods, including the baseline described in sec-

tion 3.2, the fine-tune method that fine-tunes the model on new data, the Joint-T that denotes an upper-bound by training the model on all data seen so far.

5.3. Forgetting and Generalization Evaluation

From Fig. 3(a), we can see the forgetting trend during the training process. Directly fine-tuning leads to catastrophic forgetting, LwF mitigated but still far from expectations, and our baseline with filtering mechanism improves greatly, clearly indicating that class-overlap is an issue to be addressed. JPL outperforms other methods, also the ones that uses the replay memory, demonstrating the effectiveness of our method. To verify that our method can continuously improve the model’s generalization ability, at each stage, we evaluate the model on the entire hold-off testing data. As shown in Fig. 3(b), our method achieves the best performance compared with the other competitive methods. The performance of our method doesn’t decrease at all and even increase during the entire training process. This demonstrates our method suffers from little knowledge forgetting and can further acquire new knowledge from new data.

5.4. Comparative Results with Different Settings

We report the comparative results of the methods using the three-stage CIP-ReID setting. Note that at each stage, we test the model on all encountered cameras. Consider that the camera addition sequences is agnostic, Table 2 reports the results with two different input camera orders. To verify that our method is effective in general scenarios, Table 4 additionally reports the results when there are more seen IDs than unseen IDs. We summarize the results as follows:

- On both Market-1501 and MSMT17, our method out-

Table 2. Comparison of the test mAP and R@1 on Market1501 using three stages CIP-ReID setting with two different camera addition orders. At each stage, the models are evaluated on a joint set of testing data of the cameras encountered so far. Joint-T refers to the upper-bound result. † means the exemplar-based method uses the replay memory.

Methods	Reference	Market1501 ₁						Market1501 ₂					
		Stage1		Stage2		Stage3		Stage1		Stage2		Stage3	
		mAP	R@1	mAP	R@1	mAP	R@1	mAP	R@1	mAP	R@1	mAP	R@1
Joint-T	-	71.7	87.0	71.9	85.5	74.4	88.5	69.9	82.1	72.1	85.7	73.5	88.2
Fine-tune	-	71.7	87.0	53.7	74.6	40.3	63.4	69.9	82.1	56.3	74.1	45.8	70.9
LwF	TPAMI17	71.7	87.0	57.6	77.6	49.1	71.5	69.9	87.1	61.0	77.8	58.6	79.6
AKA	CVPR21	70.1	86.7	59.8	79.7	48.2	70.3	69.1	82.0	57.3	79.8	60.4	79.7
AGD	CVPR22	71.7	87.0	57.7	77.2	44.8	67.7	69.9	82.1	58.9	76.7	52.3	74.6
PTKP†	AAAI22	71.3	87.3	66.9	82.2	63.9	81.3	69.3	81.8	68.1	83.3	68.3	84.3
Baseline	Ours	71.7	87.0	64.1	81.8	55.0	76.6	69.9	82.1	67.1	81.8	62.0	80.8
JPL		71.7	87.0	69.4	84.8	69.7	84.5	69.9	82.1	70.8	83.8	68.6	85.1

Table 3. Comparison of the test mAP and R@1 on MSMT17. The test setup is consistent with Table 2.

Methods	MSMT17					
	Stage1		Stage2		Stage3	
	mAP	R@1	mAP	R@1	mAP	R@1
Joint-T	47.2	71.6	46.5	70.1	46.2	69.4
Fine-tune	47.2	71.6	35.5	59.3	34.1	59.5
LwF	47.2	71.6	36.1	60.5	26.9	51.6
AKA	46.8	70.9	36.5	54.9	31.7	48.5
AGD	47.2	71.6	39.9	63.7	32.7	56.8
PTKP†	48.0	71.6	42.9	67.8	35.2	60.7
Baseline	47.2	71.6	40.2	64.8	32.9	58.0
JPL	47.2	71.6	44.9	69.2	41.1	66.9

Table 4. Performance with the case when there are more seen IDs than unseen IDs

Methods	Market1501 ₃					
	Stage1		Stage2		Stage3	
	mAP	R@1	mAP	R@1	mAP	R@1
Joint-T	79.4	91.1	79.1	90.6	79.9	91.2
LwF	79.4	91.1	70.7	85.0	60.9	81.8
AKA	80.4	90.3	58.4	78.6	46.6	67.3
AGD	79.4	91.1	71.8	83.4	62.8	85.5
PTKP†	79.3	91.0	77.0	87.3	70.4	85.7
Baseline	79.4	91.1	75.8	86.2	67.6	85.5
JPL	79.4	91.1	78.3	89.7	71.8	88.1

performs other state-of-the-art methods at each encountered stage, and is the closest to the upper bound Joint-T method. The superiority of our method becomes more significant as the incremental training phase proceeds.

- Surprisingly, our baseline method outperforms the state-of-the-art methods AKA and AGD, the reason for their poor performance lies in confirmation bias by misalignment of unknown classes from the new data.
- The order of camera sequences impacts the perfor-

mance to some extent, depending on the differences between cameras, the degree of class overlap, etc.

- Intuitively, more seen IDs should alleviate catastrophic forgetting, however, Table 4 shows that when the cross-camera pairwise labels are not aligned correctly, current methods still achieve worse results.

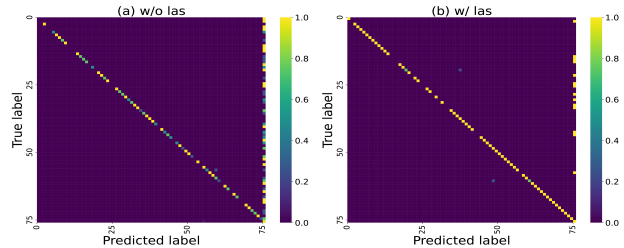


Figure 4. The normalized confusion matrices evaluating the effective of our ID-wise label assignment strategy.

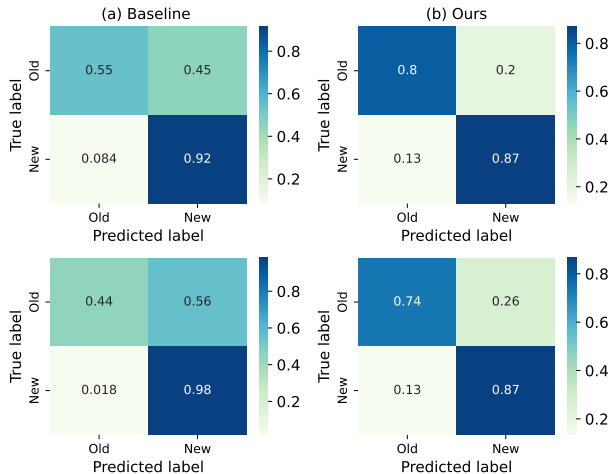
5.5. Ablation Study

A closer look at ID-wise label assignment strategy. To further observe the behavior in the ID-wise label assignment strategy (las), we plot the normalized confusion matrix with and without that strategy in Fig. 4. Specifically, in the second stage, we randomly sample total of 640 images from Market-1501, including 74 seen classes and 20 unseen classes. For easier evaluation, we uniformly use label 75 to denote all of the new classes. The diagonal entries represent the correction predictions and other entries represent the wrong prediction. Obviously, the matrix without the ID-wise label assignment strategy is more confusing, while the misclassification was alleviated by our strategy.

The effective of the OVA detector. In Fig. 5, we compare our method against the simplify filtering mechanism proposed in baseline, to validate the efficacy of the OVA detector in detecting the seen classes. As we can see, although both two methods can achieve promising results

Table 5. The ablation study of combining different loss functions

Method	\mathcal{L}_{SD}	\mathcal{L}_{Inter}	Market1501 ₁				MSMT17			
			Stage2		Stage3		Stage2		Stage3	
			mAP	R@1	mAP	R@1	mAP	R@1	mAP	R@1
Baseline w/o filtering	✗	✗	57.6	77.6	49.1	71.5	36.1	60.5	26.9	51.6
Baseline w/ filtering	✗	✗	64.1	81.8	55.0	76.6	40.2	64.8	32.9	58.0
Baseline+OVA	✗	✗	66.4	83.8	62.3	80.5	41.6	65.4	34.5	62.9
Baseline+OVA+Inter-PL	✗	✓	67.1	84.0	64.9	82.2	42.1	65.7	34.8	63.3
Baseline+OVA+SD	✓	✗	68.1	84.3	66.8	82.7	43.8	50.5	39.2	65.8
Baseline+OVA+SD+Inter-PL	✓	✓	69.4	84.8	69.7	84.5	44.9	69.2	41.1	66.9

Figure 5. The confusion matrix of the old/new classes detection results on Market1501₁(top) and MSMT17(bottom)

in recall, almost half of the samples were misclassified as new classes using the baseline method, particularly on MSMT17, while our method greatly reduce the misclassification. This demonstrates that the OVA detector is more effective and robust to discrimination the seen or unseen person.

The contribution of the loss terms. We conduct ablation studies to investigate the contribution of the loss terms. We first compare the baseline with and without the simplify filtering mechanism against a modified form using the OVA detector. As the \mathcal{L}_{intra} is also be used in baseline, we evaluate the performance gain brought by the additional \mathcal{L}_{Inter} . As shown in Table 5, the results on Market-1501 between baseline w/ and w/o the filtering operation demonstrate that without separating the old and the new classes can significantly harm the performance. However, the filtering mechanism perform poorly when processing a more difficult dataset (MSMT17). On this basic, utilizing the OVA detector achieves better performance than the baseline. Besides, both the similarity distillation and inter-domain plasticity learning can further improve the performance and the combined form achieves the best mAP/Rank-1.

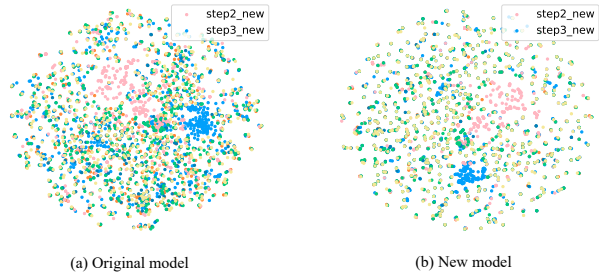


Figure 6. t-SNE visualization of feature distribution among different cameras from the original model and the new model (stage3). Different colors represent features of different cameras.

5.6. Visualization

We report a qualitative analysis showing the feature space learned by our joint plasticity learning objective on Market-1501. Fig. 6 shows the feature distribution of different cameras in different colors. Generally, the feature distributions are more cluttered using the original model, while they are more tightly grouped using our method. This shows that the new model can achieve better generalization ability on unseen classes. The features extracted by the original model have a domain gap between the original cameras and new cameras, while this can be alleviated by optimizing our joint plasticity learning objective.

6. Conclusion

In this paper, we come up with a new yet very practical task, i.e., Camera Incremental person ReID (CIP-ReID). We particularly emphasize the class-overlap issue brought by CIP-ReID where the new camera may contain identities seen before and the ideal global cross-camera annotations are absent. To approach this task, we design a novel framework called JPL-ReID. The JPL-ReID exploits a one-vs-all detector combined with an ID-wise relabel strategy to achieve the global pseudo label assignment. In addition, a joint plasticity learning objective serves as the guide to facilitate learning more generalisable representations. Extensive experiments show the effectiveness of our method.

References

- [1] Dengpan Fu, Dongdong Chen, Jianmin Bao, Hao Yang, Lu Yuan, Lei Zhang, Houqiang Li, and Dong Chen. Unsupervised pre-training for person re-identification. In *Proceedings of the IEEE Conference on Computer Vision and Pattern Recognition (CVPR)*, 2021. 2
- [2] Yang Fu, Yunchao Wei, Guanshuo Wang, Yuqian Zhou, Honghui Shi, and Thomas S Huang. Self-similarity grouping: A simple unsupervised cross domain adaptation approach for person re-identification. In *proceedings of the IEEE international conference on computer vision (ICCV)*, 2019. 2
- [3] Wenhong Ge, Junlong Du, Ancong Wu, Yuqiao Xian, Ke Yan, Feiyue Huang, and Wei-Shi Zheng. Lifelong person re-identification by pseudo task knowledge preservation. In *Proceedings of the AAAI Conference on Artificial Intelligence (AAAI)*, 2022. 2, 6
- [4] Wenhong Ge, Chunyan Pan, Ancong Wu, Hongwei Zheng, and Wei-Shi Zheng. Cross-camera feature prediction for intra-camera supervised person re-identification across distant scenes. In *Proceedings of the 29th ACM International Conference on Multimedia (ACMMM)*, 2021. 2
- [5] Kaiming He, Xiangyu Zhang, Shaoqing Ren, and Jian Sun. Deep residual learning for image recognition. In *Proceedings of the IEEE Conference on Computer Vision and Pattern Recognition (CVPR)*, 2016. 6
- [6] Lingxiao He, Xingyu Liao, Wu Liu, Xinchen Liu, Peng Cheng, and Tao Mei. Fastreid: A pytorch toolbox for general instance re-identification. *arXiv preprint arXiv:2006.02631*, 2020. 4
- [7] Shuting He, Hao Luo, Pichao Wang, Fan Wang, Hao Li, and Wei Jiang. Transreid: Transformer-based object re-identification. In *Proceedings of the IEEE International Conference on Computer Vision (ICCV)*, 2021. 1
- [8] Geoffrey Hinton, Oriol Vinyals, Jeff Dean, et al. Distilling the knowledge in a neural network. *arXiv preprint arXiv:1503.02531*, 2015. 2
- [9] Saihui Hou, Xinyu Pan, Chen Change Loy, Zilei Wang, and Dahua Lin. Learning a unified classifier incrementally via re-balancing. In *Proceedings of the IEEE Conference on Computer Vision and Pattern Recognition (CVPR)*, 2019. 1
- [10] Junkai Huang, Chaowei Fang, Weikai Chen, Zhenhua Chai, Xiaolin Wei, Pengxu Wei, Liang Lin, and Guanbin Li. Trash to treasure: Harvesting ood data with cross-modal matching for open-set semi-supervised learning. In *Proceedings of the IEEE International Conference on Computer Vision (ICCV)*, 2021. 4
- [11] Zhipeng Huang, Zhizheng Zhang, Cuiling Lan, Wenjun Zeng, Peng Chu, Quanzeng You, Jiang Wang, Zicheng Liu, and Zheng-jun Zha. Lifelong unsupervised domain adaptive person re-identification with coordinated anti-forgetting and adaptation. *arXiv preprint arXiv:2112.06632*, 2021. 1
- [12] Sergey Ioffe and Christian Szegedy. Batch normalization: Accelerating deep network training by reducing internal covariate shift. In *International conference on machine learning (ICML)*, 2015. 6
- [13] Muhammad Abdullah Jamal and Guo-Jun Qi. Task agnostic meta-learning for few-shot learning. In *Proceedings of the IEEE Conference on Computer Vision and Pattern Recognition (CVPR)*, 2019. 2
- [14] Wei Li, Rui Zhao, Tong Xiao, and Xiaogang Wang. Deepreid: Deep filter pairing neural network for person re-identification. In *Proceedings of the IEEE conference on computer vision and pattern recognition (CVPR)*, 2014. 1
- [15] Zhizhong Li and Derek Hoiem. Learning without forgetting. *IEEE transactions on pattern analysis and machine intelligence (TPAMI)*, 2017. 1, 3, 6
- [16] Yichen Lu, Mei Wang, and Weihong Deng. Augmented geometric distillation for data-free incremental person reid. In *Proceedings of the IEEE/CVF Conference on Computer Vision and Pattern Recognition (CVPR)*, pages 7329–7338, 2022. 2, 6
- [17] Hao Luo, Wei Jiang, Xuan Zhang, Xing Fan, Jingjing Qian, and Chi Zhang. Alignedreid++: Dynamically matching local information for person re-identification. *Pattern Recognition*, 2019. 2
- [18] Nan Pu, Wei Chen, Yu Liu, Erwin M Bakker, and Michael S Lew. Lifelong person re-identification via adaptive knowledge accumulation. In *Proceedings of the IEEE Conference on Computer Vision and Pattern Recognition (CVPR)*, 2021. 1, 2, 6
- [19] Roger Ratcliff. Connectionist models of recognition memory: constraints imposed by learning and forgetting functions. *Psychological review*, 1990. 1
- [20] Sylvestre-Alvise Rebuffi, Alexander Kolesnikov, Georg Sperl, and Christoph H Lampert. icarl: Incremental classifier and representation learning. In *Proceedings of the IEEE conference on Computer Vision and Pattern Recognition (CVPR)*, 2017. 1
- [21] Kuniaki Saito and Kate Saenko. Ovanet: One-vs-all network for universal domain adaptation. In *Proceedings of the IEEE International Conference on Computer Vision (ICCV)*, 2021. 2
- [22] Florian Schroff, Dmitry Kalenichenko, and James Philbin. Facenet: A unified embedding for face recognition and clustering. In *Proceedings of the IEEE conference on computer vision and pattern recognition (CVPR)*, 2015. 1, 4
- [23] Jifei Song, Yongxin Yang, Yi-Zhe Song, Tao Xiang, and Timothy M Hospedales. Generalizable person re-identification by domain-invariant mapping network. In *Proceedings of the IEEE conference on Computer Vision and Pattern Recognition (CVPR)*, 2019. 1
- [24] Yifan Sun, Liang Zheng, Yi Yang, Qi Tian, and Shengjin Wang. Beyond part models: Person retrieval with refined part pooling (and a strong convolutional baseline). In *Proceedings of the European conference on computer vision (ECCV)*, 2018. 2
- [25] Xiaoyu Tao, Xiaopeng Hong, Xinyuan Chang, Songlin Dong, Xing Wei, and Yihong Gong. Few-shot class-incremental learning. In *Proceedings of the IEEE Conference on Computer Vision and Pattern Recognition (CVPR)*, 2020. 6

- [26] Longhui Wei, Shiliang Zhang, Wen Gao, and Qi Tian. Person transfer gan to bridge domain gap for person re-identification. In *Proceedings of the IEEE conference on computer vision and pattern recognition (CVPR)*, 2018. 1, 5
- [27] Guile Wu and Shaogang Gong. Generalising without forgetting for lifelong person re-identification. In *Proceedings of the AAAI Conference on Artificial Intelligence (AAAI)*, 2021. 1, 2
- [28] Guile Wu, Xiatian Zhu, and Shaogang Gong. Tracklet self-supervised learning for unsupervised person re-identification. In *Proceedings of the AAAI Conference on Artificial Intelligence (AAAI)*, 2020. 2
- [29] Tong Xiao, Hongsheng Li, Wanli Ouyang, and Xiaogang Wang. Learning deep feature representations with domain guided dropout for person re-identification. In *Proceedings of the IEEE conference on computer vision and pattern recognition (CVPR)*, 2016. 1
- [30] Hong-Xing Yu, Ancong Wu, and Wei-Shi Zheng. Cross-view asymmetric metric learning for unsupervised person re-identification. In *Proceedings of the IEEE international conference on computer vision (ICCV)*, 2017. 2
- [31] Hong-Xing Yu, Ancong Wu, and Wei-Shi Zheng. Unsupervised person re-identification by deep asymmetric metric embedding. *IEEE transactions on pattern analysis and machine intelligence (TPAMI)*, 42(4), 2018. 2
- [32] Qing Yu, Daiki Ikami, Go Irie, and Kiyoharu Aizawa. Multi-task curriculum framework for open-set semi-supervised learning. In *European Conference on Computer Vision (ECCV)*, 2020. 4
- [33] Chi Zhang, Nan Song, Guosheng Lin, Yun Zheng, Pan Pan, and Yinghui Xu. Few-shot incremental learning with continually evolved classifiers. In *Proceedings of the IEEE Conference on Computer Vision and Pattern Recognition (CVPR)*, 2021. 2
- [34] Junyin Zhang, Yongxin Ge, Xinqian Gu, Boyu Hua, and Tao Xiang. Self-supervised pre-training on the target domain for cross-domain person re-identification. In *Proceedings of the 29th ACM International Conference on Multimedia (ACMMM)*, 2021. 2
- [35] Bo Zhao, Shixiang Tang, Dapeng Chen, Hakan Bilen, and Rui Zhao. Continual representation learning for biometric identification. In *Proceedings of the IEEE Winter Conference on Applications of Computer Vision (WACV)*, 2021. 1
- [36] Liang Zheng, Liyue Shen, Lu Tian, Shengjin Wang, Jingdong Wang, and Qi Tian. Scalable person re-identification: A benchmark. In *Proceedings of the IEEE international conference on computer vision (ICCV)*, 2015. 1, 5
- [37] Fei Zhu, Xu-Yao Zhang, Chuang Wang, Fei Yin, and Cheng-Lin Liu. Prototype augmentation and self-supervision for incremental learning. In *Proceedings of the IEEE Conference on Computer Vision and Pattern Recognition (CVPR)*, 2021. 1, 5
- [38] Kuan Zhu, Haiyun Guo, Zhiwei Liu, Ming Tang, and Jinqiao Wang. Identity-guided human semantic parsing for person re-identification. In *European Conference on Computer Vision (ECCV)*, 2020. 1
- [39] Xiangping Zhu, Xiatian Zhu, Minxian Li, Vittorio Murino, and Shaogang Gong. Intra-camera supervised person re-identification: A new benchmark. In *Proceedings of the IEEE International Conference on Computer Vision Workshops (ICCV)*, 2019. 2
- [40] Yang Zou, Xiaodong Yang, Zhiding Yu, BVK Kumar, and Jan Kautz. Joint disentangling and adaptation for cross-domain person re-identification. In *Proceedings of the European conference on computer vision (ECCV)*, 2020. 2